Total Precipitable Water Measurements from GOES Sounder Derived Product Imagery

JOHN F. DOSTALEK

Cooperative Institute for Research in the Atmosphere, Colorado State University, Fort Collins, Colorado

TIMOTHY J. SCHMIT

Advanced Satellite Products Team, Office of Research and Applications, NOAA/NESDIS, Madison, Wisconsin

(Manuscript received 18 November 1999, in final form 30 May 2001)

ABSTRACT

Statistics are compiled comparing calculations of total precipitable water (TPW) as given by GOES sounder derived product imagery (DPI) to that computed from radiosonde data for the 12-month period March 1998–February 1999. In order to investigate the impact of the GOES sounder data, these results are evaluated against statistics generated from the comparison between the first guess fields used by the DPI (essentially Eta Model forecasts) and the radiosonde data. It is found that GOES data produce both positive and negative results. Biases in the first guess are reduced for moist atmospheres, but are increased in dry atmospheres. Time tendencies in TPW as measured by the DPI show a higher correlation to radiosonde data than does the first guess. Two specific examples demonstrating differences between the DPI and Eta Model forecasts are given.

1. Introduction

The United States radiosonde network, with twice-daily launches at 0000 and 1200 UTC, and with a spacing of about 400 km between stations, is limited in its ability to depict atmospheric changes, both in space and in time (Browning 1980; Mostek et al. 1986). This limitation is particularly problematic for a forecaster concerned with predicting changes that occur over short time intervals and over small regions. For example, during the Severe Environmental Storms and Mesoscale Experiment, two studies (Kocin et al. 1986; Moore 1982) concluded that radiosonde observations taken every 3 h, and with a spacing of at most a few hundred kilometers were necessary to resolve the changes in the temperature, moisture, and wind distributions that preceded the Wichita Falls tornado outbreak on 10–11 April 1979. Some remotely sensed observations, however, are available to the forecaster more frequently in time and with higher spatial resolution than the conventional upper air observations. Geostationary Operational Environmental Satellite (GOES; Menzel and Purdom 1994) data are of particular importance to the forecaster monitoring those events that have high resolutions in space and time. GOES images have resolutions on the order of kilometers and cover the entire continental United States up to eight times per hour.

Most forecasters are familiar with the GOES imager data and its capabilities, but perhaps fewer forecasters recognize the usefulness of the GOES sounder data (Menzel et al. 1998) in tracking atmospheric changes. Certainly, information from the sounder may be employed in the forecasting process indirectly, through assimilation into a numerical model. The National Centers for Environmental Prediction's (NCEP) operational Eta Model began routinely assimilating retrieved layers of moisture from the *GOES-8* sounder in October 1997 (Lin et al. 1996; Menzel et al. 1998). Another indirect use of sounder data is the monitoring of numerical model performance. Hayden et al. (1996) mention that derived product imagery can be used to detect a timing or phase error in a numerical model forecast, and Rabin et al. (1991) compared GOES Visible and Infrared Spin Scan Radiometer Atmospheric Sounder and Special Sensor Microwave/Imager data to output from NCEP's Nested Grid Model (NGM). A more direct use of GOES sounder data in forecasting comes from derived product imagery (DPI).

Three parameters currently available as DPI are total precipitable water, lifted index, and surface skin temperature, which are produced on an hourly basis at approximately 30-km spatial (nadir) resolution. Thus the DPI can help to fill the spatial and temporal gaps in the radiosonde network. One limitation of these products, however, is that their creation is restricted to cloud-free areas. Regions that are too

Corresponding author address: John F. Dostalek, Research Associate, CIRA, Colorado State University, W. Laporte Ave., Fort Collins, CO 80523-1375.
E-mail: dostalek@cira.colostate.edu

TABLE 1a. The 0000 UTC DPI–radiosonde TPW statistics: spring, Mar–May 1998; summer, Jun–Aug 1998; fall, Sep–Nov 1998; and winter, Dec 1998–Feb 1999.

	Spring	Summer	Fall	Winter
N	2566	1327	1468	1053
$\text{Mean}_{(\text{raob})}$ (mm)	18.0	29.5	20.1	10.5
Bias (mm)	−1.8	−0.2	−0.2	−0.3
σ (mm)	3.3	4.6	3.8	2.7
r	0.94	0.91	0.94	0.94

N = number of comparisons. σ = standard deviation. r = correlation coefficient.

TABLE 1b. Same as in Table 1a, but for 1200 UTC DPI–radiosonde TPW statistics.

	Spring	Summer	Fall	Winter
N	2102	1117	1247	832
$\text{Mean}_{(\text{raob})}$ (mm)	16.7	28.0	19.1	9.7
Bias (mm)	−1.4	−0.6	−0.2	−0.2
σ (mm)	3.3	4.2	3.6	2.2
r	0.93	0.94	0.95	0.96

cloudy to retrieve the above three parameters are used to create a fourth DPI, cloud-top pressure. Another weakness of the DPI is the relative lack of vertical resolution due to the broad weighting functions from the sounder instrument. As a result, integrated parameters such as total precipitable water (TPW) will tend to be more accurate than individual level measurements, such as the 500-hPa dewpoint temperature (Rao and Fuelberg 1998). Future geostationary sounding instruments with high spectral resolution (i.e., interferometers) will help improve vertical resolution.

This paper assesses the quality of the *GOES-8* TPW DPI, and gives two examples of their applicability in monitoring temporal and spatial gradients of total precipitable water. The paper is divided into three sections. Section 2 begins with a brief overview of the GOES sounder DPI. It continues with a statistical comparison of the TPW DPI as derived from the *GOES-8* sounder and TPW generated from radiosonde observations for the 12-month period between March 1998 and February 1999. These statistics are compared to those derived from comparing the first guess field TPW to the radiosonde TPW. Two brief examples are presented in section 3 to illustrate the utility of the GOES sounder derived TPW. The paper concludes with a summary in section 4.

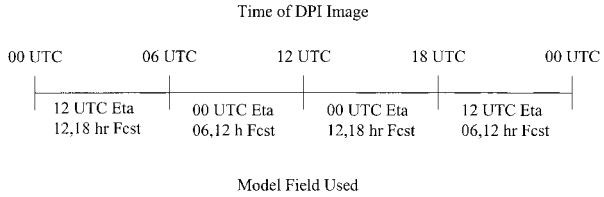

FIG. 1. Eta Model forecasts from which first guess soundings are used in DPI production.

2. Derived product imagery

a. Description

Derived product imagery are "image presentations of meteorological products, . . . of the imager or sounder" (Hayden et al. 1996). The DPI discussed here are created every hour from the sounder temperature and moisture profiles, generated using a nonlinear, simultaneous, physical retrieval algorithm (Ma et al. 1999). The retrieval algorithm uses a background (first guess) state of the atmosphere derived from 6- to 18-h Eta Model forecasts (Rogers et al. 1996; Black et al. 1993). The Eta Model field acquired has a horizontal grid spacing of 80 km, which is interpolated to a 1° latitude × 1° longitude grid. The vertical grid spacing is 50 hPa. The model forecasts are spatially interpolated to the latitude and longitude of the clear field of view used in the retrieval. The forecasts are linearly interpolated to the nearest hour of the satellite data. For example, between 0000 and 0600 UTC, the first guess uses fields valid between 12 and 18 h after the 1200 UTC model run (Fig. 1). A first guess skin temperature is also derived, using calculations involving infrared window measurements and historical radiosonde observations. Hourly surface data are used as boundary conditions for the retrieval algorithm. Finally, the forward integration of the radiative transfer operates on a fixed set of pressure intervals, but is bounded by the earth's surface.

b. Statistical comparison between DPI, first guess, and radiosonde derived TPW

Of interest is how well the TPW DPI correspond to, or to what degree they differ from, those values derived from radiosonde measurements. Before presenting the statistics, however, a few comments will be made concerning the comparison between the GOES DPI and radiosonde measurements. First, satellite measurements are representative of a volume of the atmosphere, whereas radiosonde data are point values. Also, the satellite and radiosonde measurements are not necessarily concurrent in time or space; in this study, however, they are required to be within 1 h, and 33 km, of each other.

→

FIG. 2. (a) The 0000 UTC total precipitable water DPI vs total precipitable water from radiosonde for Mar 1998–Feb 1999. Solid line is one-to-one correspondence, and dashed line is least squares fit. Total precipitable water units are mm. (b) As in (a) but for 1200 UTC data.

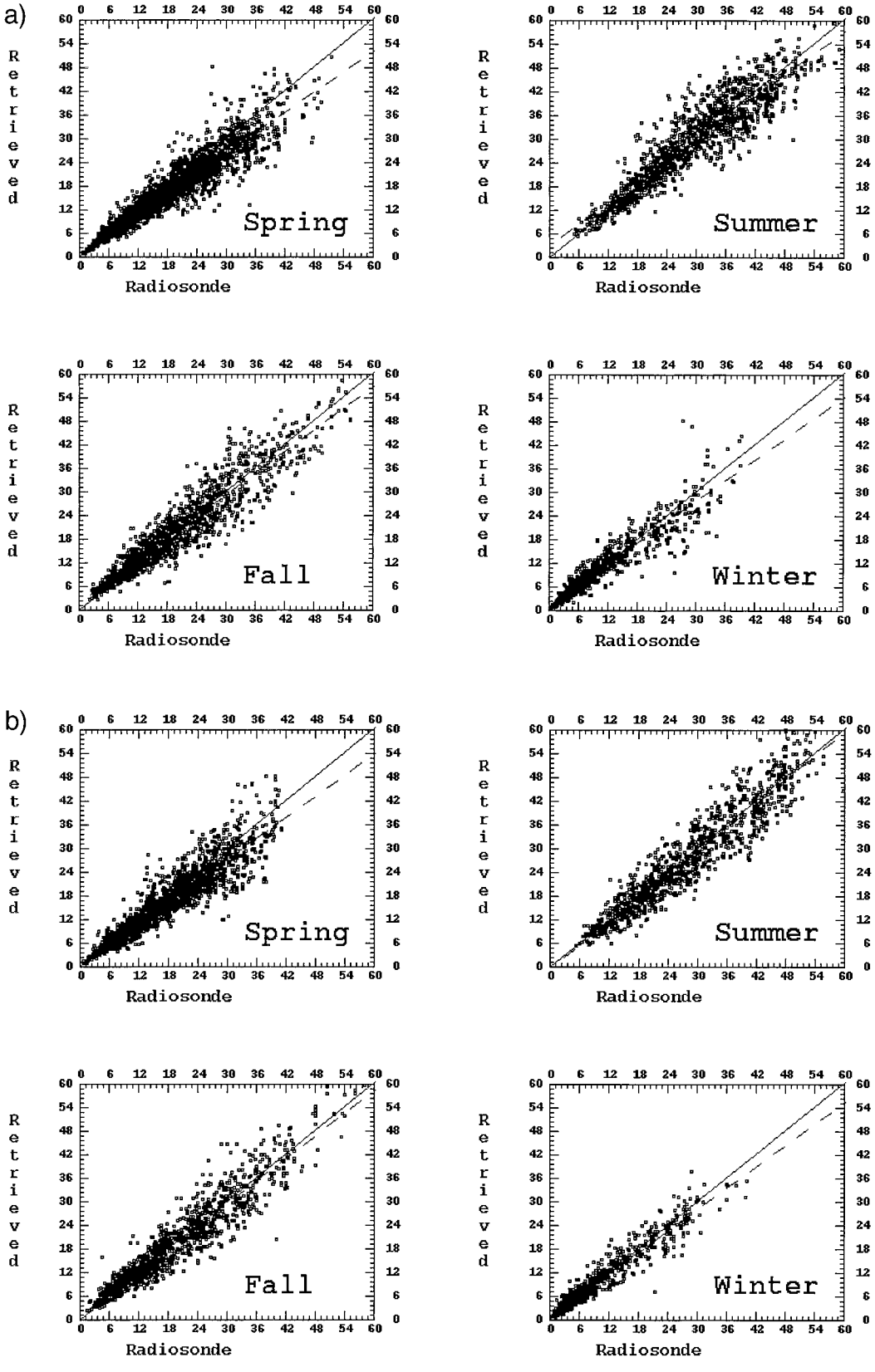
a)
Retrieved
Radiosonde
Spring
Summer
Fall
Winter
b)
Retrieved
Radiosonde
Spring
Summer
Fall
Winter

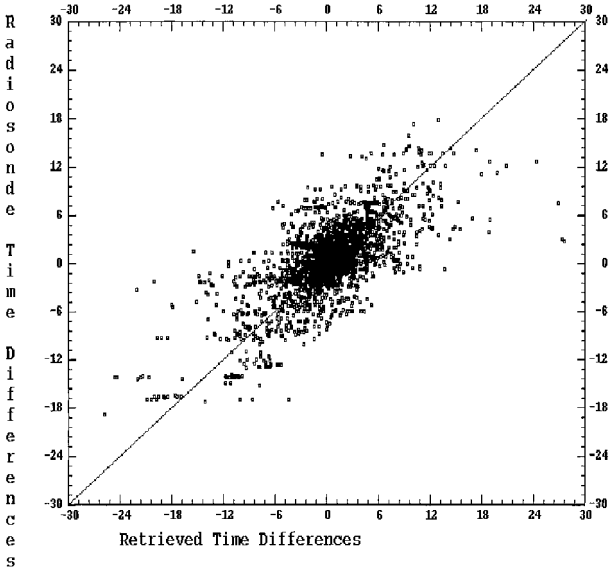

FIG. 3. Twelve-hour time tendency comparison of DPI and radiosonde total precipitable water for the period Mar 1998–Feb 1999 (in mm). Number of comparisons is 2384.

TABLE 2a. Same as in Table 1a but for 0000 UTC first guess–radiosonde TPW statistics.

	Spring	Summer	Fall	Winter
N	2566	1327	1468	1053
Mean$_{(raob)}$ (mm)	18.0	29.5	20.1	10.5
Bias (mm)	−1.0	−1.1	−0.3	−0.1
σ (mm)	3.6	4.5	3.7	2.6
r	0.93	0.91	0.94	0.95

TABLE 2b. Same as in Table 1a but for 1200 UTC first guess–radiosonde TPW statistics.

	Spring	Summer	Fall	Winter
N	2102	1117	1247	832
Mean$_{(raob)}$ (mm)	16.7	28.0	19.1	9.7
Bias (mm)	−0.9	−1.5	−0.3	−0.1
σ (mm)	3.4	4.4	3.6	2.4
r	0.93	0.93	0.95	0.95

Finally, the assumed ''truth'' of radiosonde measurements is itself suspect (Pratt 1985; Schmidlin 1988). In spite of these concerns, radiosonde data provide a consistent means of validation, and have been used previously in the literature for this purpose (Ma et al. 1999; Rao and Fuelberg 1998). In this study comparisons of DPI TPW were made to corresponding 0000 and 1200 UTC radiosonde profile calculations for 12 months of data, including the spring (Mar–May) of 1998, the summer (Jun–Aug) of 1998, the fall (Sep–Nov) of 1998, and the winter (Dec–Feb) of 1998/99.

Tables 1a and 1b contain the number of comparisons (N), the mean radiosonde TPW, the bias (computed as $\text{TPW}_{\text{DPI}} - \text{TPW}_{\text{raob}}$), the standard deviation (σ), and the correlation coefficient (r) for each season at 0000 and 1200 UTC, respectively, for the TPW. The biases are less than 2 mm, and standard deviations less than 5 mm. When viewed in the context of the mean TPW, these data show that during the wetter seasons of summer and fall, the biases are at a minimum (absolute value), yet the standard deviations are at a maximum. Conversely, during the drier

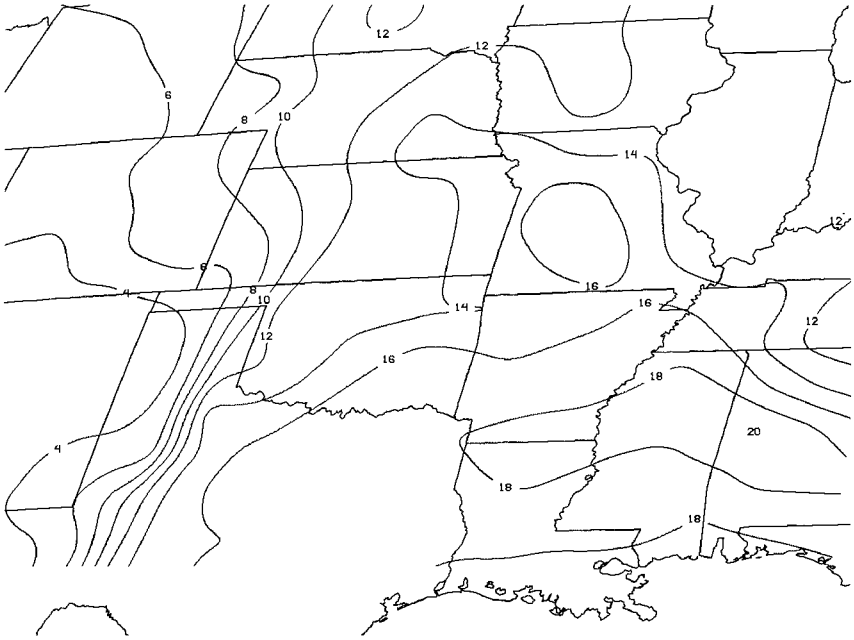

FIG. 4. Contours of surface mixing ratio (g kg^{-1}) for 1700 UTC 17 Jun 1998.

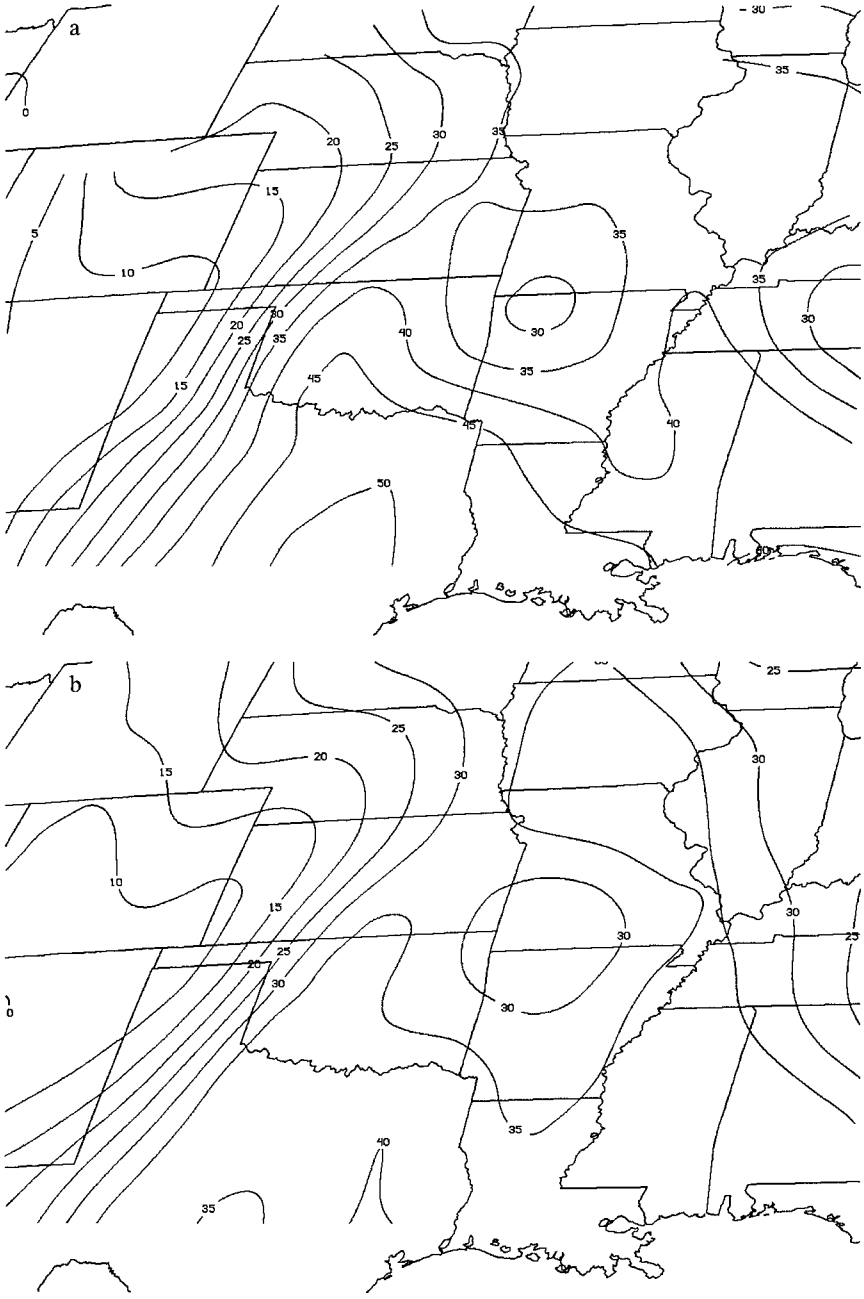

FIG. 5. (a) *GOES-8* TPW DPI from 1647 UTC 17 Jun 1998; (b) 1200 UTC Eta Model forecast valid 1700 UTC 17 Jun 1998.

TABLE 3a. Difference in the values listed in Tables 1a and 2a, where Δ is the difference in absolute value of the quantities, i.e., $\Delta = |\,|_{\text{DPI}} - |\,|_{\text{first guess}}$.

	Spring	Summer	Fall	Winter
N	—	—	—	—
$\text{Mean}_{(\text{raob})}$ (mm)	—	—	—	—
ΔBias (mm)	0.8	−0.9	−0.1	0.2
$\Delta\sigma$ (mm)	−0.3	0.1	0.1	0.1
Δr	0.1	0.0	0.0	−0.1

TABLE 3b. Same as in Table 3a but using the difference between the values in Tables 1b and 2b.

	Spring	Summer	Fall	Winter
N	—	—	—	—
$\text{Mean}_{(\text{raob})}$ (mm)	—	—	—	—
ΔBias (mm)	0.5	−0.9	−0.1	0.1
$\Delta\sigma$ (mm)	−0.1	−0.2	0.0	−0.2
Δr	0.0	0.1	0.0	0.1

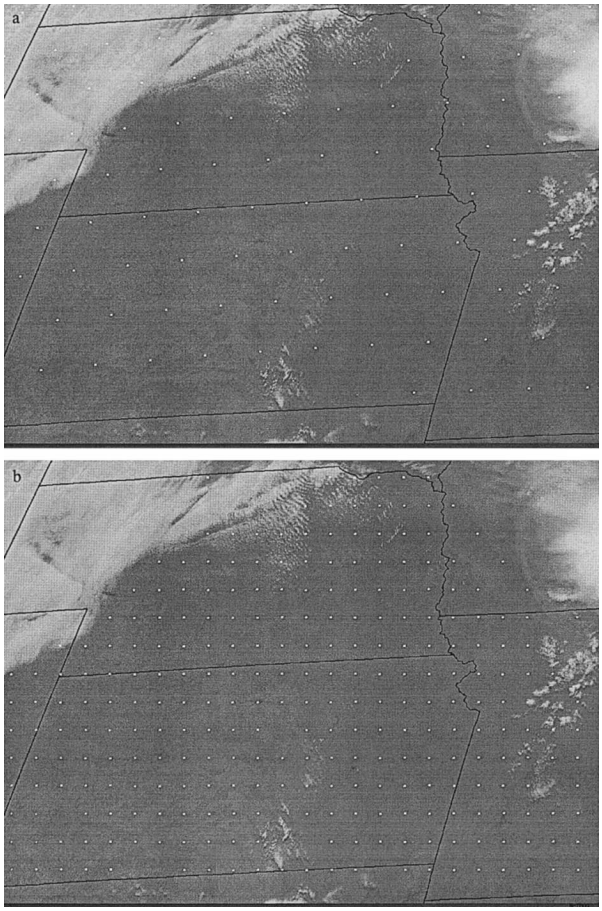

FIG. 6. (a) Data points for Eta Model on an 80-km grid. (b) Data points of *GOES-8* DPI for 1647 UTC 17 Jun 1998.

TABLE 4a. DPI–radiosonde TPW statistics for 0000 and 1200 UTC for the entire 12-month period, for radiosonde values of TPW greater than or equal to 20 mm and for radiosonde values of TPW greater than or equal to 35 mm.

	Radiosonde ≥ 20 mm	Radiosonde ≥ 35 mm	Total
N	2901	737	11 565
$\text{Mean}_{(\text{raob})}$ (mm)	30.3	41.6	19.0
Bias (mm)	−1.5	−1.9	−0.8
σ (mm)	4.6	5.3	3.5
r	0.86	0.72	0.96

TABLE 4b. Same as in Table 4a but for first guess–radiosonde TPW statistics.

	Radiosonde ≥ 20 mm	Radiosonde ≥ 35 mm	Total
N	2901	737	11 565
$\text{Mean}_{(\text{raob})}$ (mm)	30.3	41.6	19.0
Bias (mm)	−1.7	−3.3	−0.7
σ (mm)	4.6	5.1	3.6
r	0.84	0.68	0.95

TABLE 4c. Difference in values listed in Tables 4a and 4b, where Δ is the difference in absolute value of the quantities, i.e., $\Delta = |\ |_{\text{DPI}} - |\ |_{\text{first guess}}$.

	Radiosonde ≥ 20 mm	Radiosonde ≥ 35 mm	Total
N	—	—	—
$\text{Mean}_{(\text{raob})}$ (mm)	—	—	—
Bias (mm)	−0.2	−1.4	0.1
σ (mm)	0.0	0.2	−0.1
Δr	0.2	0.4	0.1

winter and spring seasons, the biases are at a maximum and the standard deviations are at a minimum. The correlation coefficients remain around 0.94, with a reduction to 0.91 for the 0000 UTC summer observations. The relationship among the mean TPW, the bias, and the standard deviation as depicted graphically (Figs. 2a and 2b) confirm the tabulated results. The least squares fit, given by the dashed line, generally lies below the one-to-one correspondence, shown as a solid line, implying a negative bias in the DPI TPW. The difference between the slopes of the two lines is greater in the winter and spring than in the summer and fall, corresponding to the greater biases found for those two seasons. Additionally, the spread of the data points increases with increasing TPW. This behavior also agrees with the larger standard deviations present for greater TPW.

Statistics were also compiled between the first guess field and the radiosonde values of TPW (Tables 2a and 2b). In order to show how the DPI improve or degrade the first guess TPW, the differences between the absolute values of the numbers in Table 1a (Table 1b) and Table 2a (Table 2b) were computed and are shown in Table 3a (Table 3b). As biases and standard deviations decrease, the closer the relationship is between two sets of data. Therefore, negative numbers in the bias and standard deviation rows of Table 3 mean that the DPI improved upon the first guess. Conversely, an increase in the correlation coefficient implies a closer relationship between two sets of data. Positive values imply an improvement upon the first guess by the DPI. The data show mixed results, only three of which are consistent improvements or degradations. The DPI reduce the bias of the first guess in the summer and fall, yet increase the bias in the winter and spring. The DPI also produce a reduction in the standard deviation in the spring.

Because areas of greater TPW are associated with more significant precipitation events than those with lower TPW, further comparisons were made among the DPI, the first guess, and radiosonde measurements for instances where the radiosonde-measured TPW was greater than or equal to 20 mm and greater than or equal to 35 mm (0000 and 1200 UTC measurements, and all seasons combined) (Tables 4a–c). Under these conditions, the DPI both reduce the biases and increase the correlation coefficients from the first guess. However,

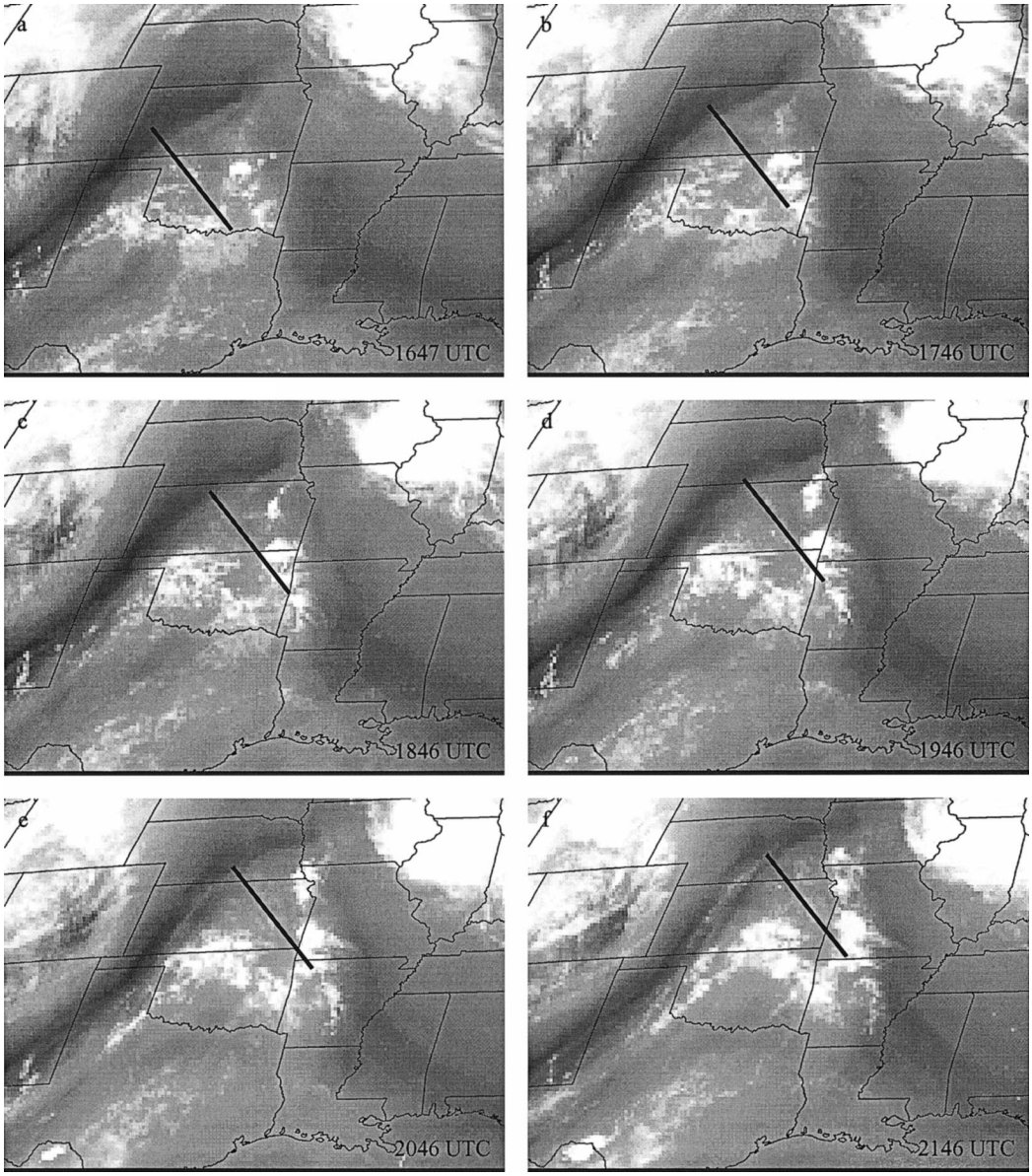

FIG. 7. *GOES-8* 7.43-μm image sequence from 17 Jun 1998. Solid lines denote the approximate positions of the axis of the moisture pulse discussed in the text.

the standard deviation shows no change for the 20-mm lower limit and an increase of 0.2 for the 35-mm limit. Equivalent statistics were evaluated for the 12-month period as a whole and are included in the last columns of Tables 4a–c. Reflecting the changes as viewed within each season, the results are mixed, with the DPI reducing the standard deviation and increasing the correlation coefficient, yet also increasing the bias.

The ability of the DPI to capture temporal trends was also evaluated. Twelve-hour changes (0000–1200 UTC and 1200–0000 UTC) in TPW were compared to the corresponding radiosonde values for the entire 12-month period, a total of 2384 observations (Fig. 3). Corresponding temporal trends were also computed using the first guess and radiosonde values of TPW. The changes in DPI TPW show a 0.71 correlation with the radiosonde TPW changes, a 0.12 improvement over the 0.59 correlation of the first guess TPW changes with the radiosonde TPW changes.

The above findings are in agreement with those of Rao and Fuelberg (1998), who examined the quality of *GOES-8* retrievals with respect to radiosonde profiles, using a linear, simultaneous, physical retrieval algorithm similar to that described by Hayden (1988). Their study included data from August to November 1995 and used the NGM forecast fields as a basis for the first guess.

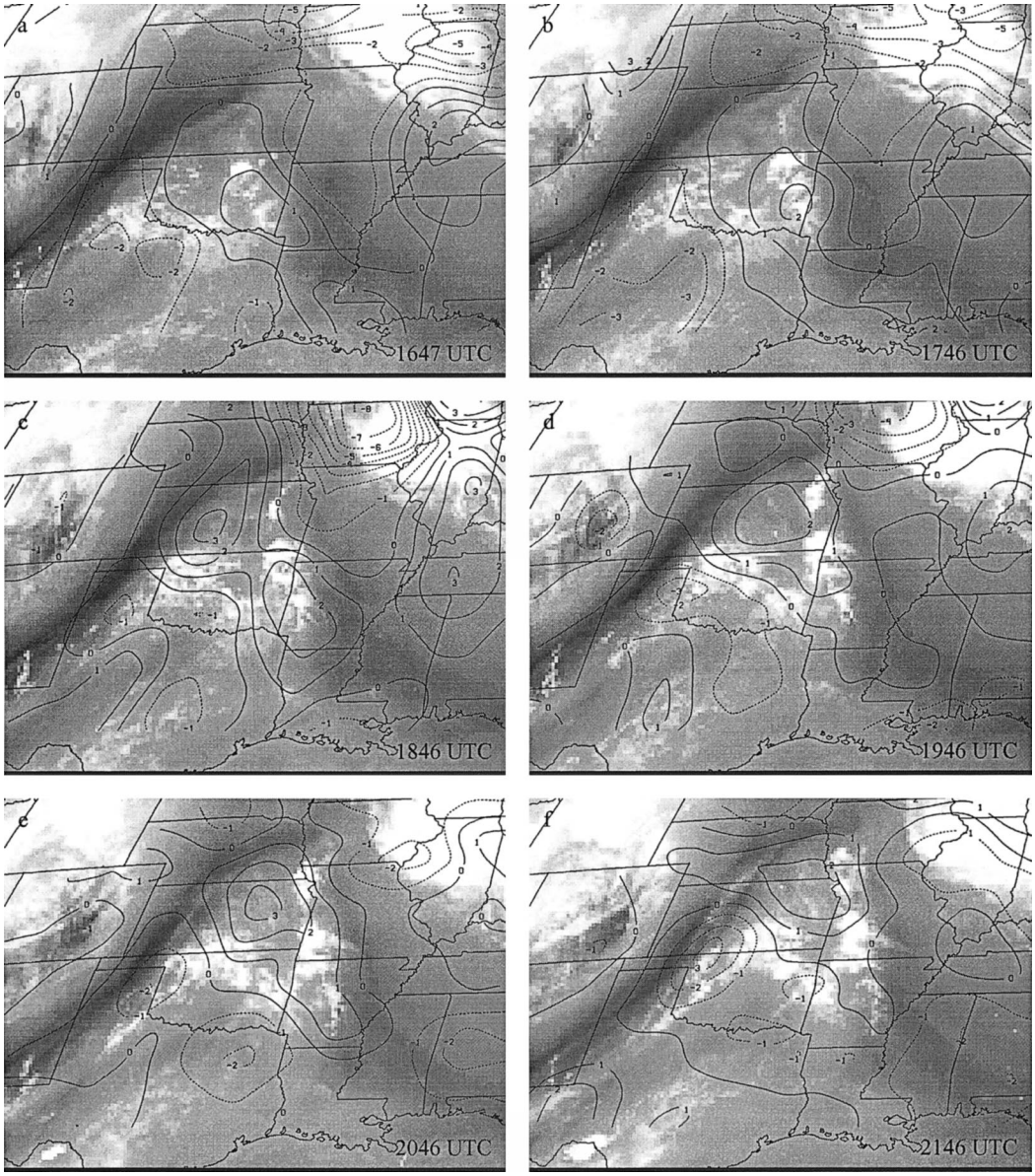

FIG. 8. Hourly differences in DPI TPW (mm): (a) 1647–1546, (b) 1746–1647, (c) 1846–1746, (d) 1946–1846, (e) 2046–1946, and (f) 2146–2046 UTC. Satellite images are the same as in Fig. 7.

In their study, it was found that the *GOES-8* TPW retrieval improved upon the first guess TPW more often than not. Specifically, the *GOES-8* retrieval improved the first guess 48% of the time, degraded the first guess 31% of the time, and did not change the first guess 21% of the time.

Although the changes to the first guess are small, and not guaranteed to be closer to reality, a few comments need to be made. First of all, the comparisons are being made over the data-rich continental United States, where the forecast models would be expected to perform their best. It could be that the additional GOES data added to the first guess would have an even greater impact in data-void regions, oceans and the Gulf of Mexico, for example, as shown by Ma et al. (1999). Second, information from the sounder is already included in the first guess, in the form of layered precipitable water in the numerical model analysis. Third, the spatial and temporal gradients afforded by the GOES sounder should add valuable information to the forecaster. Finally, forecasters from the Western Region of the National Weather Service (NWS) have used sounder products experimentally since 1996. Schrab (1998) has documented several cases where the sounder TPW DPI as well as lifted index DPI were very useful in real-time forecasting and nowcasting. The GOES sounder DPI will be disseminated

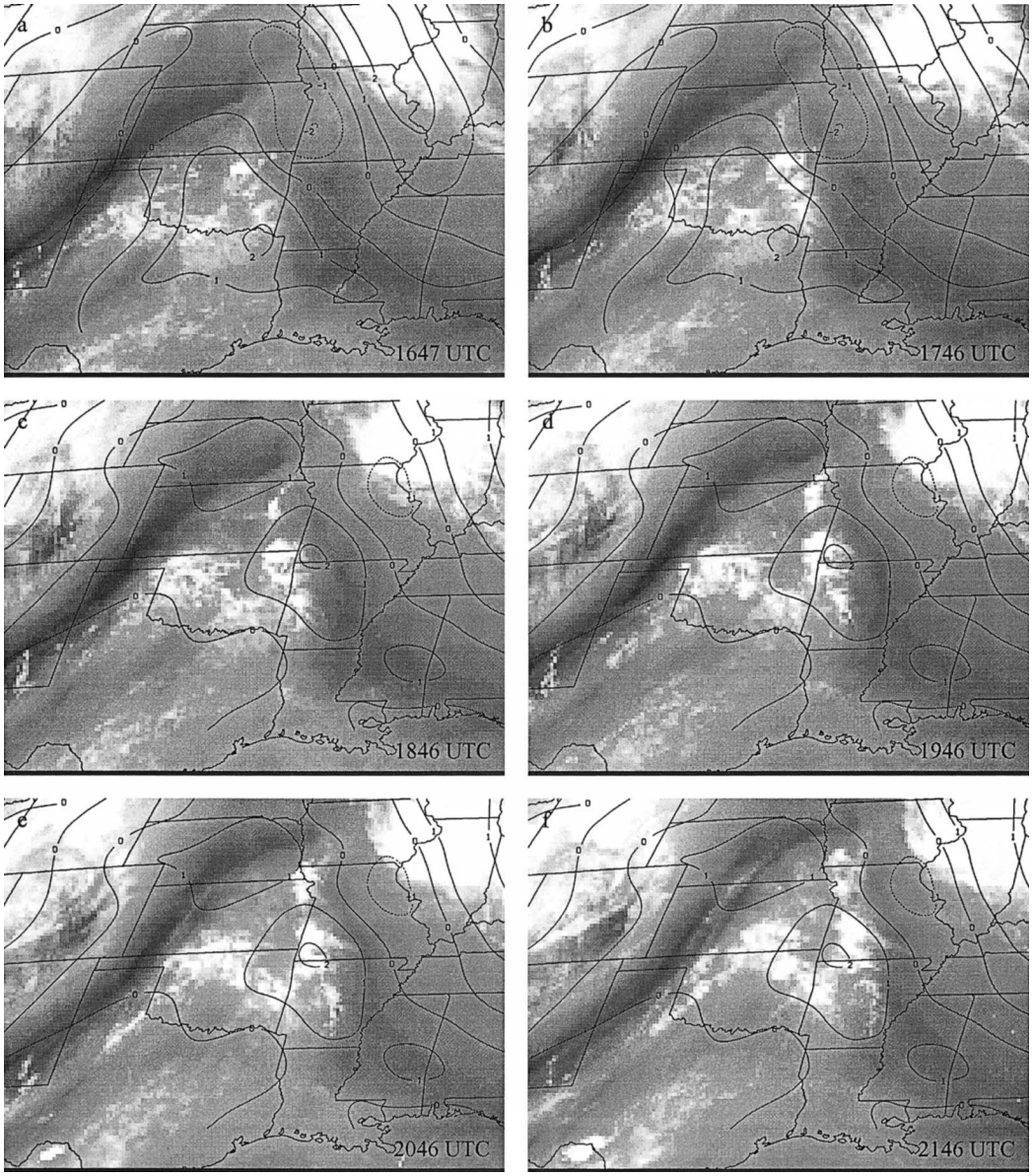

FIG. 9. Hourly differences in Eta Model forecast TPW (mm). (a), (b) Hourly difference between 1200 and 1800 UTC. (c)–(f) Hourly difference between 1800 and 0000 UTC 18 Jun 1998. Satellite images are the same as in Fig. 7. Note that because the Eta Model used has output every 6 h, the hourly differences will be equal between forecast validation times.

via the Advanced Weather Interactive Processing System (AWIPS) system to NWS forecasters.

c. Comments on the horizontal resolutions of the Eta Model and the GOES DPI

The Eta Model is being run at increasingly finer horizontal grid spacing (currently 32 km with plans to change to 22 km). As already mentioned, the DPI have a resolution of 30 km $\times$ 30 km at nadir. The claim, then, that the DPI can add information to the Eta Model concerning the spatial gradients of TPW needs to be explained. Among other considerations, the ability of a forecast model to accurately predict the weather depends on the ''grid spacing'' of the data assimilated into the run. When considering the vertical structure of the atmosphere, radiosonde data provide the most consistent information to numerical models. The grid spacing of the United States radiosonde network is roughly 400 km. As previously mentioned, GOES-derived layered precipitable water has been assimilated into the Eta Model since 1997 to help fill some of the gaps in the radiosonde network. But the layered precipitable water product is available only in cloud-free regions. So, for

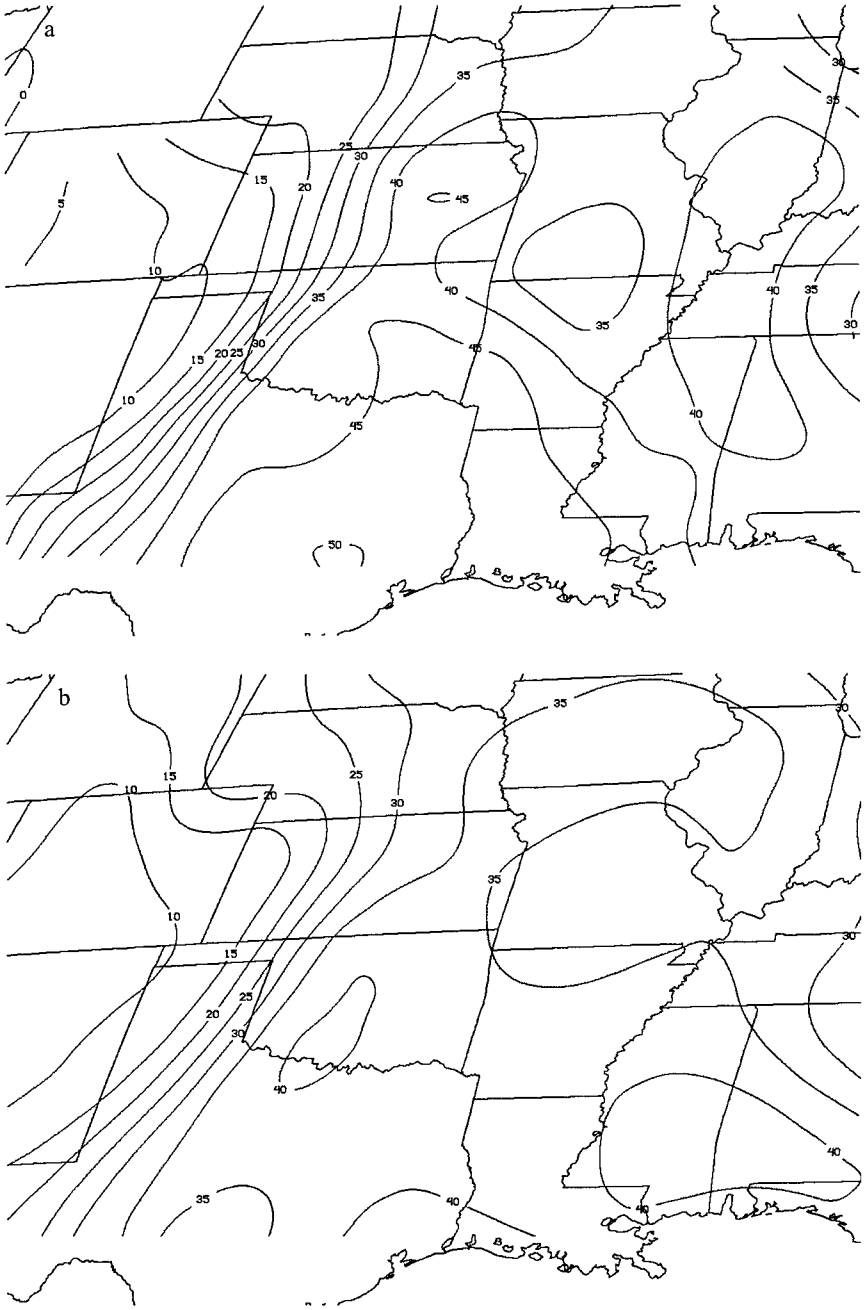

FIG. 10. (a) *GOES-8* TPW DPI from 2146 UTC 17 Jun 1998; (b) 1200 UTC Eta Model forecast valid at 2200 UTC 17 Jun 1998.

example, if a cloud deck exists over a portion of the United States during the data assimilation period, the vertical moisture structure of the atmosphere is only determined at the radiosonde sites. But if the deck dissipates later in the day, the GOES gets a second chance to add information about the TPW in the form of DPI. Although this information has a grid spacing that is coarser than the Eta Model, it is still finer than that of the data assimilated into the model run, that is, 400 km between radiosonde sites.

Even when the GOES-derived layered precipitable water data are able to fill the voids between radiosonde sites for assimilation into the model run, its impact on the model is at a horizontal spacing of around 50 km, as the precipitable water for this purpose is measured using a 5×5 pixel array. In addition, the Eta Model disseminated to AWIPS, the standard platform used by National Weather Service forecasters, is interpolated from a 32-km grid to an 80-km grid. Thus, the 3×3 pixel array of the DPI should still be able to add valuable information concerning

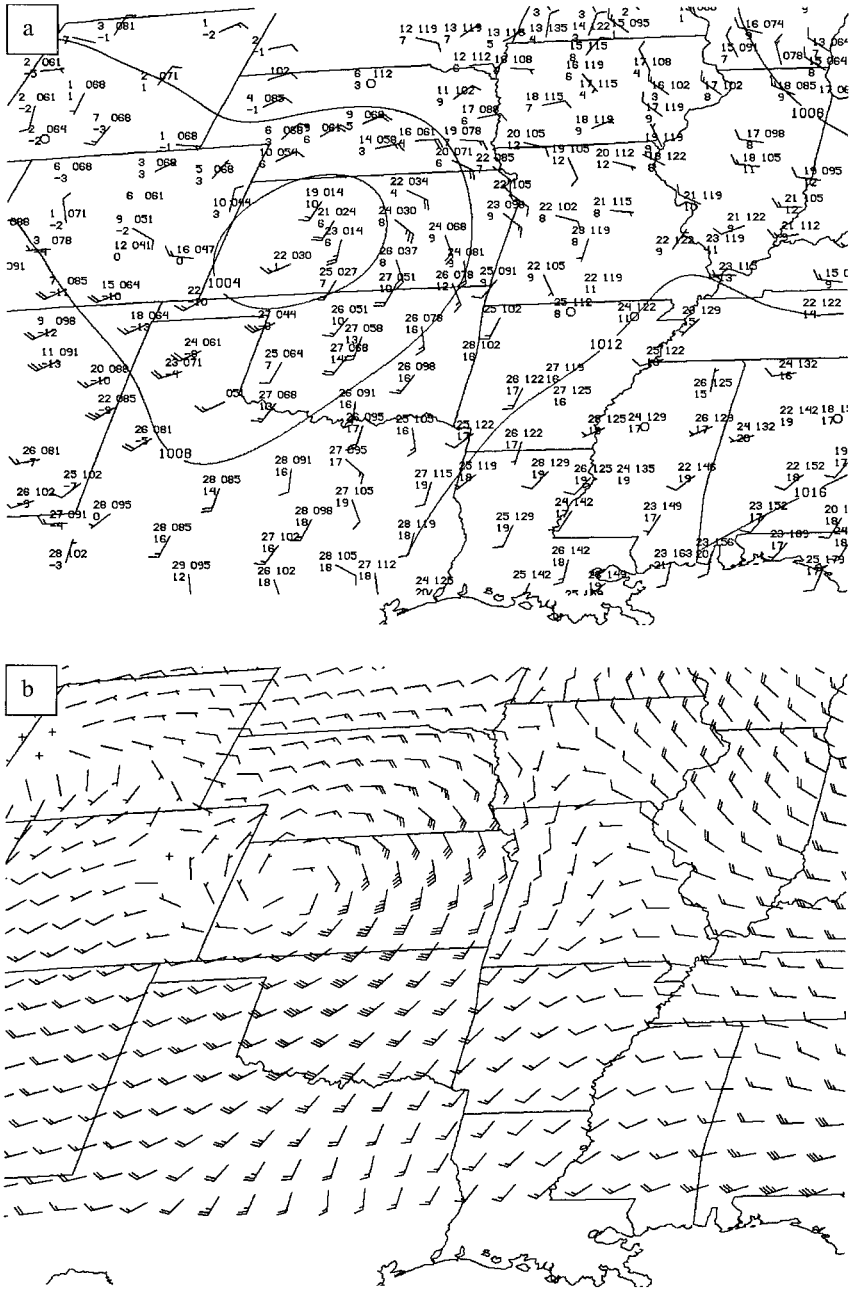

FIG. 11. (a) Surface observations for 1800 UTC 14 Apr 1998. Station model values clockwise from upper left are temperature in °C, altimeter setting in tenths of hPa, with leading 9 or 10 omitted, and dewpoint temperature in °C. Contours of altimeter setting in hPa. (b) The 1200 UTC Eta Model 850-hPa wind vectors valid at 1800 UTC 14 Apr 1998. For both (a) and (b), half barb is equal to 2.5 m s^{-1}, full barb is equal to 5 m s^{-1}.

the spatial distribution and gradients of TPW to the Eta Model forecast. Improvement in the accuracy in the temporal distributions of TPW in time are also possible, as GOES soundings are available every hour for the production of DPI; Eta Model forecasts are available every 6 h on AWIPS. The next section provides two examples where the improved spatial and temporal resolutions afforded by the TPW DPI are evident.

3. Two examples

a. 17 June 1998

An opportunity for assessing the ability of the DPI to resolve spatial and temporal gradients of TPW is present in the sharp moisture contrast, called the dryline environment, which often exists during the spring in the west-central United States. In these situations, a dry air

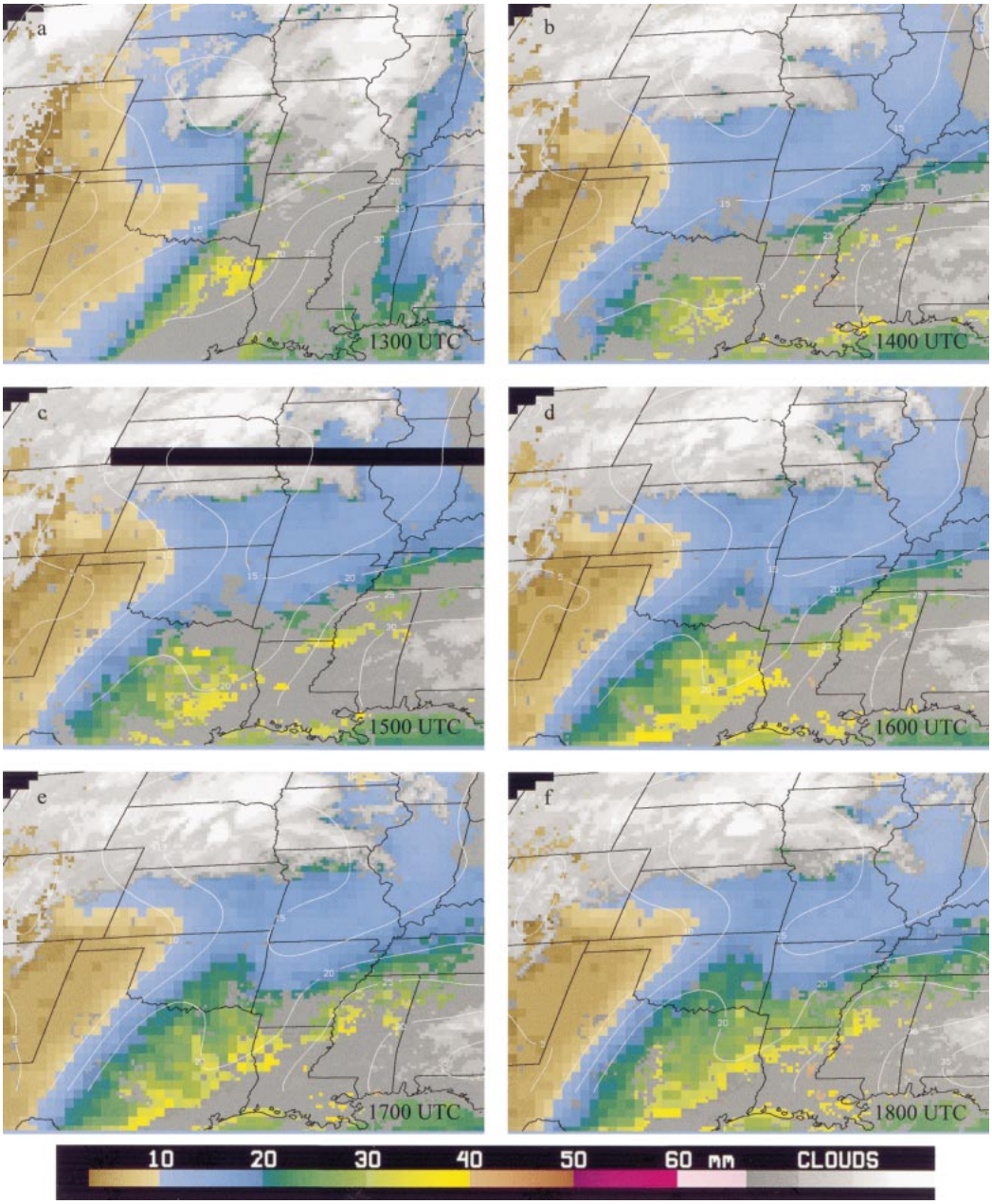

FIG. 12. Time sequence from (a) 1300 UTC 14 Apr 1998 to (l) 0000 UTC 15 Apr 1998 of *GOES-8* TPW DPI with contours of Eta Model forecast TPW (mm). Time at lower right corresponds to the Eta Model forecast. Time of the GOES DPI is approximately 15 min earlier.

mass over the Rockies and high plains lies adjacent to an air mass over the central United States that is characterized by moist low levels (Schaefer 1986). This west to east moisture gradient can be seen both in the surface mixing ratio field, and in the total precipitable water field.

The atmosphere exhibited such a juxtaposition of air masses on 17 June 1998, where the surface mixing ratio field shows enhanced moisture gradients from western Kansas to western Texas at 1700 UTC (Fig. 4). Coincident with the surface mixing ratio gradients, both the GOES DPI and the Eta Model forecast show enhanced TPW gradients (Fig. 5). Because the transition between air masses is abrupt, higher-resolution datasets offer improved ability to monitor any changes that occur. The difference in the number of data points between the 80-km output of the Eta Model on AWIPS and the 1647 UTC GOES DPI is demonstrated in Fig. 6, which shows observations over the Kansas–Nebraska region, overlaid on a GOES visible image. This figure also underscores

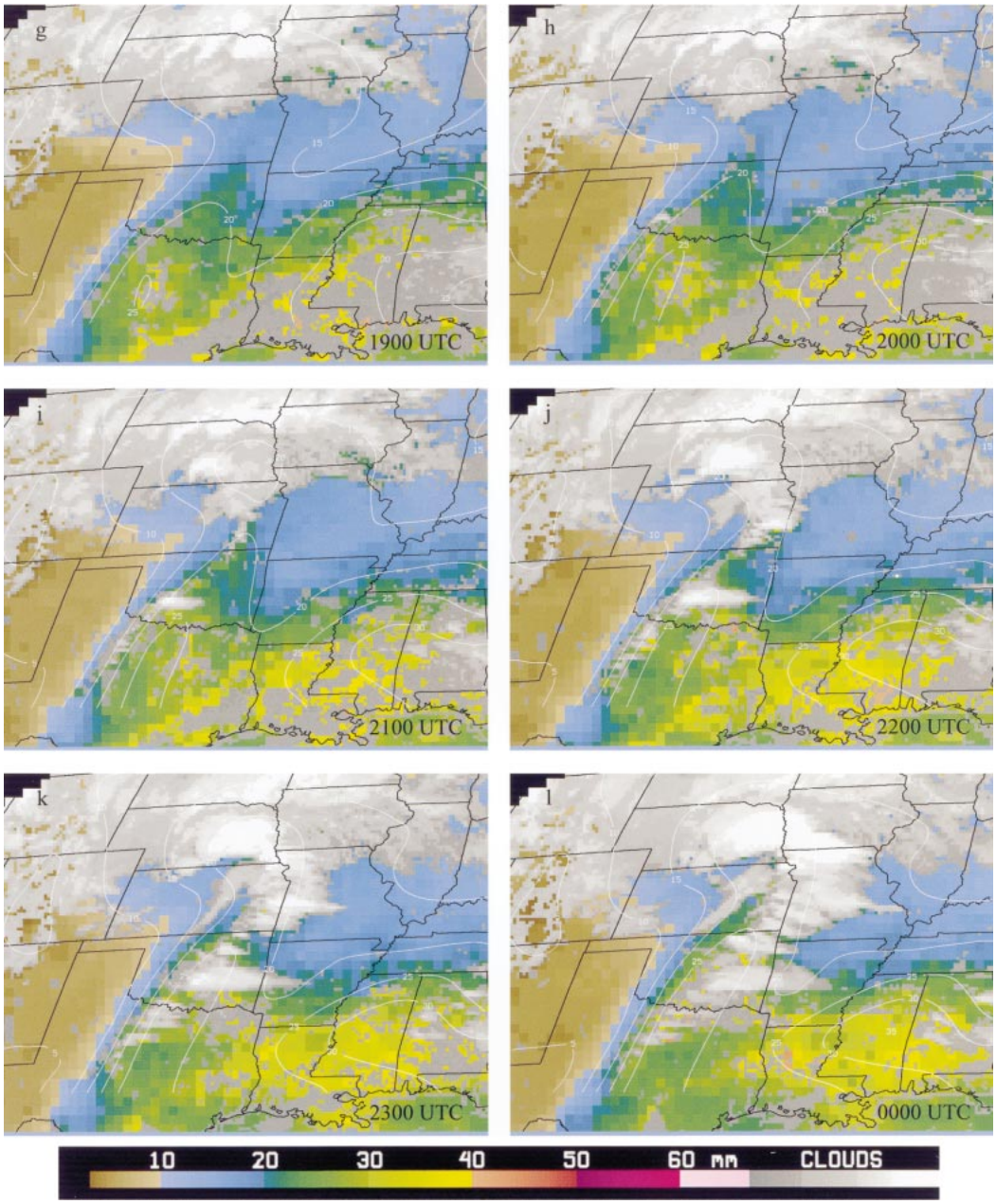

FIG. 12. (*Continued*)

a shortcoming of the TPW product. Infrared sensors such as the GOES sounder cannot retrieve temperature and moisture profiles in cloudy areas and, therefore, offer no TPW information at those points.

Although the DPI TPW gradient extends over a greater horizontal distance than the Eta's, the two gradients are qualitatively similar in magnitude and location. Subsequent analyses, however, demonstrate differences between the Eta and DPI. A time sequence of images from the *GOES-8* 7.43-μm sounder channel, which is sensitive to low-level moisture, shows a ridge of water vapor moving from southwest to northeast along the gradient of moisture (Fig. 7). Because the TPW DPI is a sounder product, one would assume that it would capture a feature such as that shown in Fig. 7. Indeed, a time sequence of hourly differences in TPW as measured by the DPI confirms a pulse of moisture traveling along the moisture gradient (Fig. 8). A similar sequence of hourly differences computed by the Eta Model forecast also shows the pulse of moisture (Fig. 9), but its progression to the northeast is not as well depicted. In particular, note that the dry slot (dark band extending from southeastern New Mexico to southeastern Nebraska)

seen in the satellite imagery evolves from a straight feature to an elongated S over time, as the pulse of moisture travels to the northeast. The inflection point of the S corresponds to a change from an increase in moisture over time to a decrease in moisture over time as the pulse moves over a point. The gradient of change in TPW as measured by the DPI is qualitatively well placed with respect to the inflection point of the S, particularly after 1746 UTC. The corresponding contours of TPW as measured by the Eta Model do not compare as well with the satellite imagery. Admittedly, this example might be interpreted as GOES data confirming GOES data. From a different perspective, however, it could be stated that a qualitative feature noted in satellite imagery corresponds to a quantitative feature in the DPI to a degree not matched by the model forecast.

The two distributions of TPW at the end of the image sequence give additional insight into the performance of the DPI in comparison to the Eta forecast. One of the characteristics of the springtime moisture gradient of the Great Plains is an increase in magnitude during the afternoon (Rhea 1966; Schaeffer 1986). In comparing the 2146 UTC contours of DPI TPW (Fig. 10a) with those of 1647 UTC (Fig. 5a), an increase in the magnitude of the TPW gradient is apparent along the dryline environment, from Kansas through Texas. The 2200 UTC contours of TPW from the Eta Model (Fig. 10b) do not show a qualitative gradient increase along the dryline environment with respect to the 1700 UTC data (Fig. 5b). The 1700 and 2200 UTC values of TPW were determined from linear interpolation between the 6-h forecast verification times.

b. 14 April 1998

A second example of the utility of the GOES DPI in monitoring spatial and temporal TPW fields is found on 14 April 1998, where southerly flow ahead of a surface low in western Kansas advected moisture northward into eastern Oklahoma and eastern Kansas (Fig. 11). In the Storm Prediction Center's 1507 UTC convective outlook for that day, the forecaster noted the following:

> VWP/PROFILER DATA SHOW 30–40 KT LOW LEVEL SSELY FLOW IN PLACE AT THE MOMENT ACROSS E TX AND OK . . . SUGGESTING THAT MOISTURE PLUME SHOULD REACH NE KS/WRN MO BY LATE TODAY/EARLY TONIGHT . . . AND THAT ETA BOUNDARY LAYER MOISTURE FIELDS ARE UNDERDONE.

The GOES DPI indicates that the TPW was farther north during the morning and afternoon than the Eta Model predicted (Fig. 12). For example, note the Eta Model's 20-mm contour line, which corresponds to the change from blue to green enhancement in the DPI, throughout the sequence of images. The Eta TPW contours have been linearly interpolated between the 6-h validation times. Although the two data sources are in general agreement after 2000 UTC, the Eta Model lagged the GOES data up to 250 km over the first 7 h.

4. Summary

With the advances in satellite instrumentation of the past decade, forecasters now have access not only to visible and infrared data from imagers, but also quantitative derived products from sounding instruments. In particular, GOES sounder DPI are currently being produced for both GOES-East and GOES-West. The DPI are derived from the GOES temperature and moisture retrievals, which are created from a nonlinear, simultaneous, physical retrieval algorithm. The DPI include a lifted index, total precipitable water, and surface skin temperature product for clear regions, and a cloud-top pressure product for cloudy areas. Because of the high spatial and temporal resolution of these products, they can help to fill the gaps between radiosonde locations and launch times. In this paper, the GOES DPI TPW product was statistically compared with radiosonde data over the period March 1998–February 1999. These results were evaluated against a statistical comparison between the first guess used by the DPI, which is based on Eta Model forecasts, and radiosonde data. The DPI showed both positive and negative impacts on the first guess. Two notable improvements made by the DPI are the reduction of first guess biases in relatively moist atmospheres, and increased accuracy in measuring time tendencies of TPW.

Two examples illustrate uses and limitations of the TPW DPI. In particular, temperature and moisture retrievals cannot be made from the GOES sounder in cloudy areas. For generally clear scenes, however, the DPI are able to monitor spatial gradients and temporal changes of TPW, as seen in the context of the Great Plains dryline environment and of the northward flow of moisture ahead of a low pressure system in the south-central United States. These features were not as well resolved by the Eta TPW forecasts. The Eta Model, to be sure, runs at a grid spacing comparable to, or even smaller than, the distance between GOES retrievals. However, it must be kept in mind that the input into the model that is relevant to TPW calculations is supplied at a grid spacing that is coarser, in both space and time, than the GOES retrievals used by the DPI. Also, the Eta Model most available to forecasters arrives via AWIPS on a grid with points spaced 80 km apart, not the Eta's native 32 km. These issues allow the GOES soundings the opportunity, in the form of DPI, to improve upon the Eta Model forecast TPW.

Acknowledgments. The thoughtful reviews of the manuscript by Drs. Mark DeMaria and Don Hillger of the NOAA/NESDIS Regional and Mesoscale Meteorology Team at CIRA were much appreciated. Dr. Stev-

en Koch and three anonymous reviewers gave additional valuable insight into ways in which the manuscript might be improved. Scott Bachmeier of the Cooperative Institute of Meteorological Satellite Studies and Gary S. Wade of NOAA/NESDIS assisted in the research presented here. This study was performed under NOAA Grant NA67RJ0152.

REFERENCES

Black, T. L., D. G. Deaven, and G. J. DiMego, 1993: The step-mountain eta-coordinate model: 80 km ''early'' version and objective verifications. NWS Tech. Procedures Bull. 412, 31 pp. [Available from Office of Meteorology, National Weather Service, 1325 East–West Highway, Silver Spring, MD 20910.]

Browning, K. A., 1980: Review of local weather forecasting. *Proc. Royal Soc. London,* **A371,** 197–211.

Hayden, C. M., 1988: GOES-VAS simultaneous temperature-moisture retrieval algorithm. *J. Appl. Meteor.,* **27,** 705–733.

——, G. S. Wade, and T. J. Schmit, 1996: Derived product imagery from *GOES-8. J. Appl. Meteor.,* **35,** 153–162.

Kocin, P. J., L. W. Uccellini, and R. A. Petersen, 1986: Rapid evolution of a jet streak circulation in a preconvective environment. *Meteor. Atmos. Phys.,* **35,** 103–138.

Lin, Y., E. Rogers, G. J. DiMego, K. E. Mitchell, and R. M. Aune, 1996: Assimilation of GOES-8 moisture data into NMC's Eta model. Preprints, *Eighth Conf. on Satellite Meteorology and Oceanography,* Atlanta, GA, Amer. Meteor. Soc., 518–520.

Ma, X. L., T. J. Schmit, and W. L. Smith, 1999: A nonlinear physical retrieval algorithm—Its application to the *GOES-8/9* sounder. *J. Appl. Meteor.,* **38,** 501–513.

Menzel, W. P., and J. F. W. Purdom, 1994: Introducing GOES-I: The first of a new generation of geostationary operational environmental satellites. *Bull. Amer. Meteor. Soc.,* **75,** 757–781.

——, F. C. Holt, T. J. Schmit, R. A. Aune, A. J. Schreiner, G. S. Wade, and D. G. Gray, 1998: Application of *GOES-8/9* soundings to weather forecasting and nowcasting. *Bull. Amer. Meteor. Soc.,* **79,** 2059–2077.

Moore, J. T., 1982: The forcing and evolution of the three dimensional moisture convergence during the 10–11 April 1979 severe weather outbreak. Preprints, *12th Conf. on Severe Local Storms,* San Antonio, TX, Amer. Meteor. Soc., 209–212.

Mostek, A., L. W. Uccellini, R. A. Petersen, and D. Chesters, 1986: Assessment of VAS soundings in the analysis of a preconvective environment. *Mon. Wea. Rev.,* **114,** 62–87.

Pratt, R. W., 1985: Review of radiosonde humidity and temperature errors. *J. Atmos. Oceanic Technol.,* **2,** 404–407.

Rabin, R. M., L. A. McMurdie, C. M. Hayden, and G. S. Wade, 1991: Monitoring precipitable water and surface wind over the Gulf of Mexico from microwave and VAS satellite imagery. *Wea. Forecasting,* **6,** 227–243.

Rao, P. A., and H. E. Fuelberg, 1998: An evaluation of *GOES-8* retrievals. *J. Appl. Meteor.,* **37,** 1577–1587.

Rhea, J. O., 1966: A study of thunderstorm formation along drylines. *J. Appl. Meteor.,* **5,** 58–63.

Rogers, E., T. L. Black, D. G. Deaven, G. J. DiMego, Q. Zhao, M. E. Baldwin, N. W. Junker, and Y. Lin, 1996: Changes to the operational ''early'' eta analysis/forecast system at the National Centers for Environmental Prediction. *Wea. Forecasting,* **11,** 391–413.

Schaefer, J. T., 1986: The dryline. *Mesoscale Meteorology and Forecasting,* P. S. Ray, Ed., Amer. Meteor. Soc., 549–570.

Schmidlin, F. J., 1988: WMO international radiosonde comparison, phase II final report: 1985. WMO Tech. Doc. WMO/TD 312, WMO, Geneva, Switzerland, 113 pp. [Available from WMO Secretariat, 41 Ave. Giuseppe Motta, Case Postale 2300, CH-1211 Geneva, Switzerland.]

Schrab, K. J., 1998: Monitoring the southwest U.S. summer monsoon using GOES-9 data. Preprints, *16th Conf. on Weather Analysis and Forecasting,* Phoenix, AZ, Amer. Meteor. Soc., 368–369.